INVERSION OF GEODETIC DATA FOR SPATIALLY VARIABLE SLIP-RATE ON THE SAN ANDREAS FAULT NEAR PARKFIELD, CA

Jessica R. Murray, Paul Segall, Peter Cervelli,
Department of Geophysics, Stanford University, Stanford, CA 94305

Will Prescott, Jerry Svarc, USGS, 345 Middlefield Rd., Menlo Park, CA 94024

INTRODUCTION

The town of Parkfield is located on the San Andreas fault in central California. Motion on the fault in this area is transitional between that in the creeping section to the northwest, where surface slip-rates are 25-30 mm/yr (*Lisowski and Prescott*, 1981), and that in the locked section to the southeast. Over the past 120 years, there have been a series of ~M6 earthquakes here with, on average, 22 years between them. Despite *Bakun and McEvilly's* 1984 prediction that the next ~M6 earthquake at Parkfield would occur in 1988 ± 5 years, the most recent of these events was in 1966, making the interseismic period between the 1966 earthquake and the present the longest yet. The 1966 event nucleated beneath Middle Mountain, which is located ~8 km northwest of the town of Parkfield, and the earlier earthquakes are thought to have nucleated in a similar location (*Bakun and McEvilly*, 1984). The 1966 earthquake ruptured unilaterally to the southeast, stopping near the town of Cholame (*Segall and Du*, 1993).

In their 1987 paper, *Harris and Segall* inverted the rates of line length change calculated from trilateration measurements made between 1959 and 1984 by the California Department of Water Resources (CDWR), the California Division of Mines and Geology (CDMG), and the USGS for the spatial distribution of slip-rate on the fault. Using a model fault plane that coincided with the 1966 rupture plane, they inferred the presence of a region of low-slip rate on the fault extending from the southeast to the area below Middle Mountain. They also saw evidence for fault normal contraction. Since their study, the USGS has collected GPS data in the Parkfield area. These newer data, collected between 1991 and 1998, are independent of the trilateration data in terms of collection method and temporal coverage, however some of the same benchmarks are represented in both datasets. *Murray et al.* (in review) discuss the results of inversions of the GPS velocities for the spatial distribution of slip-rate.

In the current paper we compare the results of inversions using trilateration data alone, GPS data alone, and a combination of trilateration and GPS data. The trilateration and GPS networks are shown in figure 1. We repeated the inversion of the trilateration data, rather than simply compare the GPS results to those of *Harris and Segall* (1987), for several reasons: 1) We have found that using non-negative least squares (NNLS) is preferable to the singular value decomposition (used by *Harris and Segall*) because it ensures uniformly right lateral slip in the solution and because it results in improved model resolution. 2) We have one more year of data (1985) and data from several additional lines not used in the *Harris and Segall* (1987) paper. 3) For each data set (trilateration, GPS, and combination) we identified the optimal transition depth (between seismogenic and freely slipping crust) and deep slip-rate based on the misfit between observed rates and those predicted by the estimated slip-rates. The deep slip-rate we used for the inversion of trilateration data is different than that

determined by *Harris and Segall*. 4) Like *Harris and Segall* (1987), we assigned uncertainties to the trilateration data based on the error analysis given in *King et al.,* (1987). However, we also scaled the uncertainties by the χ^2 of the inversion of line-length changes for line-length rates of change.

METHOD

For both GPS and trilateration data, we first used the observations to estimate rates. Following the method of *King et al.*, (1987), we used the measured line lengths for the trilateration network to solve for the constant rate of line-length change for each line. Additionally, where applicable, we solved for offsets at the time of the 1966 earthquake and the transition from CDWR to CDMG measurements. For the GPS data, we used the position measurements to solve for a constant velocity at each station.

We modeled the fault in the same way as *Harris and Segall* (1987). It consists of three segments in map view. The part of the San Andreas in the Parkfield area (which we will call the Parkfield plane) is represented by a gridded vertical fault plane 36 km long and extending from the surface to 14 km depth. It is flanked by an ungridded block 100 km long and 14 km wide to the northwest which represents the creeping section and another 100 km by 14 km block to the southeast which represents the locked section. Like the Parkfield plane, these two blocks intersect the earth's surface. A block 1000 km long and wide is centered below the Parkfield plane to represent the far-field motion of the plates at a steady deep slip-rate.

For inverting the combination of trilateration and GPS data, we set up the problem as shown below. For the inversion of EDM or GPS data alone, we used just the appropriate parts of the full system of equations,

$$\begin{bmatrix} \mathbf{v} \\ \dot{\mathbf{L}} \\ \dot{\mathbf{s}}_{constraints} \\ \mathbf{0} \end{bmatrix} = \begin{bmatrix} \mathbf{G}_{GPS} \\ \mathbf{G}_{EDM} \\ \mathbf{G}_{constraints} \\ \gamma^2\mathbf{H} \end{bmatrix} \dot{\mathbf{s}} \quad .$$

The first row relates the GPS velocities to slip-rate on the model fault through the design matrix $\mathbf{G}_{GPS}$ based on the equations given in *Okada's* 1985 paper. The second row relates the line-length rates of change to the slip-rate through $\mathbf{G}_{EDM}$ which is also based on *Okada's* paper.

The third row specifies constraints on the slip-rate for the row of blocks on the gridded fault plane that intersect the surface. We used the same constraint values as *Harris and Segall* (1987) based on data from creepmeters, alinement arrays, and short aperture networks. $\mathbf{G}_{constraints}$ is a direct mapping between these values and the estimated slip-rates. The values acted as constraints because they were assigned much lower uncertainties than the other data. We also used this method to constrain the deep slip-rate and that on the creeping section. We did not constrain the locked section.

Finally, we assumed that the slip-rate distribution is somewhat spatially smooth and implemented this using the finite difference approximation of the Laplacian operator, **H**,

weighted by a parameter γ^2. Greater values of γ lead to more emphasis on a smooth solution and a poorer fit to the data. We used cross validation (CV) to choose an optimal value for γ (*Wahba*, 1990). For each value of γ, a series of slip-rate estimates was found, each with one datum omitted. The residual between an omitted datum and that predicted by the model is the "cross-validation residual". The "cross validation sum of squares" (CVSS) is the sum of these squared residuals for a given γ. The optimal value of γ corresponds to the smallest CVSS. An estimate with too little smoothing will model noise, preventing it from adequately predicting the omitted datum. Estimates with too much smoothing will have greater misfit.

As discussed in *Harris and Segall* (1987) there is a trade-off between transition depth and deep slip-rate. The greater the depth, the greater the deep slip-rate may be. *Murray et al.* (in review) used the following method to determine the optimal combination of transition depth and deep slip-rate. They compared the minimum CVSS (that found using the optimal amount of smoothing) for damped least squares solutions spanning a range of depths and constrained deep slip-rates. The minimum CVSS occurred for a transition depth of 14 km and a deep slip-rate of 32.6 mm/yr. This value for deep slip-rate is in keeping with geologic estimates of ~33.9 ± 2.9 mm/yr (*Sieh and Jahns*, 1984). The 1966 aftershocks and background seismicity in the Parkfield area extend to depths of ~14 km (*Eaton et al., 1970; Eberhart-Phillips and Michael*, 1993), implying that slip-rate transients extend to this depth. For the NNLS inversions presented here, we used a similar method. However, performing CV using NNLS for a large number of depth/deep slip-rate combinations is computationally intensive and thus prohibitively slow. Since we were more confident in the estimate of 14 km for transition depth than in a particular deep slip-rate, we tested a range of deep slip-rates for this depth using NNLS and CV. For each dataset, we used the deep slip-rate and γ that corresponded to the lowest CVSS in the results presented below.

RESULTS

The results of inverting the trilateration data are given in figure 2. Plot (a) shows the CVSS as a function of γ and plot (b) shows the estimated slip-rate distribution. As one might expect, this distribution is very similar to that found by *Harris and Segall* (1987), exhibiting an area of low slip-rate covering much of the Parkfield plane and extending northwest to the area below Middle Mountain.

Figure 3 shows the velocities at the EDM sites based on a model coordinate solution (*Segall and Matthews*, 1988) and those predicted from the slip-rate distribution. The model coordinate solution is a means of finding the velocities for the stations at the ends of the trilateration lines based on the rates of line-length change and the geometry of the network. Since there may be arbitrary rigid body motions of the network that do not change the line-length measurements and thus cannot be resolved by the data, we must provide additional information. In the case of the model coordinate solution, one tries to make the observed velocities found from the line-length rates of change as close to those predicted by the modeled slip-rate distribution as possible. In this case, any remaining residual between the model coordinate solution velocities and the predicted velocities must be due to model misfit. Several sites have been omitted from this map because they were not adequately tied to the network. There are some sites (such as Davis, Blhllres, and Bonnie) for which there appears

to be an unmodeled component of fault normal contraction. We found this occurs for fewer sites than did *Harris and Segall* (1987).

As noted above, *Murray et al.* (in review) present the results of inversions using the GPS data. Therefore we only give a brief overview here. Figure 4a shows choice of γ made by CV and figure 4b shows the estimated slip-rate distribution. Like that estimated from the EDM data, this solution has an area of low slip-rate on the southeastern half of the Parkfield plane. However, with the GPS data, this area does not extend as far to the northwest as that found using the trilateration data. The observed and predicted GPS velocities are shown in figure 5. We have found no consistent spatial patterns in the residuals to suggest an unmodeled component of fault normal compression in the inversions of GPS data.

When estimating both the rates of line-length change and the velocities, we assume constant rates. If it is true that deformation rates have been steady over the interseismic period at Parkfield, we should be able to combine the two data sets into one inversion for slip-rate on the fault. The results of this inversion are shown in figure 6. As one might expect, the area of low slip-rate extends northwest on the fault to a point midway between the extents of low slip-rate estimated with only trilateration and only GPS data. One should note that, even after scaling, the rates of line-length change have lower uncertainties than the GPS velocities (whose uncertainties have been scaled by the χ^2 of the velocity solution). Therefore, the trilateration data have more weight in the inversion, and the resulting slip-rate distribution looks more like that found using trilateration data only than that found using GPS data alone.

Perhaps a better way of visualizing the comparison among the estimated slip-rate distributions is shown in figure 7. The top plot shows the slip-rate distribution found using EDM data minus that found using GPS data. Although the difference is close to zero for the southeastern part of the fault plane, for the northwestern portion the results based on trilateration data are distinctly lower. Interestingly, the hypocenter of the 1966 earthquake, indicated by the star, is located in the area of greatest difference, almost 18 mm/yr, between the two estimated slip-rates. The plots (b) and (c) show other comparisons that lead to the same conclusions.

DISCUSSION

Since the trilateration data and the GPS data are temporally independent, the differences among the slip-rate distributions may be indicative of a temporal change in the style of deformation in the Parkfield area.

The Coalinga earthquake in 1983 caused left-lateral surface creep on the San Andreas near Parkfield. *Simpson et al.* (1988) modeled the static stress changes arising from the New Idria (1982), Coalinga, and Kettleman Hills (1985) events and concluded that the first two imposed left lateral stress on the San Andreas over the Parkfield plane and some of the area covered by the trilateration network. One should note that the USGS trilateration measurements (which started in the 1970s for some sites and in 1980 for most) have lower uncertainties than those made by CDWR or CDMG. Thus, the trilateration data that may have been affected by the Coalinga-Kettleman Hills events are the most heavily weighted.

The GPS data cover the time period 1992 – 1994 during which there were three M4.7 earthquakes in the Parkfield area (*Fletcher and Spudich,* 1998). These events nucleated in the region of the greatest difference in slip-rate estimated from trilateration and GPS data. Thus, the GPS data may show some evidence of increased slip-rate on the fault during this time. Our investigations of the model resolution show that areas of the size that shows the significant difference in estimated slip-rate in figure 7a should be resolvable, but areas smaller than this are probably not.

CONCLUSIONS

1) The inversions of trilateration data and GPS data both image an area of low slip-rate covering more than half the area of the San Andreas fault that ruptured in the 1966 Parkfield earthquake. This is evidence that strain has been accumulating on the fault throughout the interseismic period, however it has been 34 years since the last ~M6 Parkfield event.
2) The area of low slip-rate estimated using trilateration data extends northwest to the area below Middle Mountain, where the 1966 earthquake nucleated. In contrast, the area of low slip-rate found with GPS data only extends to a point mid-way between Carr Hill and Middle Mountain.
3) That the two data sets span different time periods suggests that the differences in the estimated slip-rate could represent a temporal change in the style of deformation in the Parkfield area, perhaps related to the long interseismic period since the 1966 event and to other seismic activity during the intervening time. However, more analysis is required before adopting this conclusion.

REFERENCES

Bakun, W. H., and T. V. McEvilly, Recurrence models and Parkfield, California, earthquakes, *J. Geophys. Res., 89,* 3051-3058, 1984.

Eaton, J. P., M. E. O'Neill, and J. N. Murdock, Aftershocks of the 1966 Parkfield-Cholame, California, earthquake: a detailed study, *Bull. Seismol. Soc. Am., 60,* 4, 1151-1197, 1970.

Eberhart-Phillips, D. and A. J. Michael, Three-dimensional velocity structure, seismicity, and fault structure in the Parkfield region, central California, *J. Geophys. Res., 98,* 15,737-15,758, 1993.

Fletcher, J. B., and P. Spudich, Rupture characteristics of the three *M* ~ 4.7 (1992 – 1994) Parkfield earthquakes, *J. Geophys. Res., 103,* 835-854, 1998.

Harris, R. and P. Segall, Detection of a locked zone at depth on the Parkfield, California, segment of the San Andreas fault, *J. Geophys. Res., 92,* 7945-7962, 1987.

King, N. E., P. Segall, and W. Prescott, Geodetic measurements near Parkfield, California, 1959-1984, *J. Geophys. Res., 92,* 2747-2766, 1987.

Lisowski, M. and W. H. Prescott, Short-range distance measurements along the San Andreas fault system in central California, 1975 to 1979, *Bull. Seismol. Soc. Am., 71,* 5, 1607-1624, 1981.

Murray, J. R., P. Segall, P. Cervelli, W. Prescott, J. Svarc, Inversion of GPS data for spatially variable slip-rate on the San Andreas Fault near Parkfield, CA, *Geophys. Res. Lett.,* in review.

Okada, Y., Surface deformation due to shear and tensile faults in a half-space, *Bull. Seismol. Soc. Am., 75,* 4, 1135-1154, 1985.

Segall, P. and Y. Du, How similar were the 1934 and 1966 Parkfield earthquakes?, *J. Geophys. Res., 98,* 4527-4538, 1993.

Segall, P. and M. V. Matthews, Displacement calculations from geodetic data and the testing of geophysical deformation models, *J. Geophys. Res.*, 93, 14,954-14,966, 1988.

Sieh, K., and R. H. Jahns, Holocene activity of the San Andreas fault at Wallace Creek, California, *Geo. Soc. Am. Bull., 95,* 883-896, 1984.

Simpson, R. W., S. S. Schulz, L. D. Dietz, and R. O. Burford, The response of creeping parts of the San Andreas fault to earthquakes on nearby faults: two examples, *Pure and App. Geophys., 126,* 665-685, 1988.

Wahba, G., *Spline Models for Observational Data,* Society for Industrial and Applied Mathematics, Philadelphia, Pa., 1990.

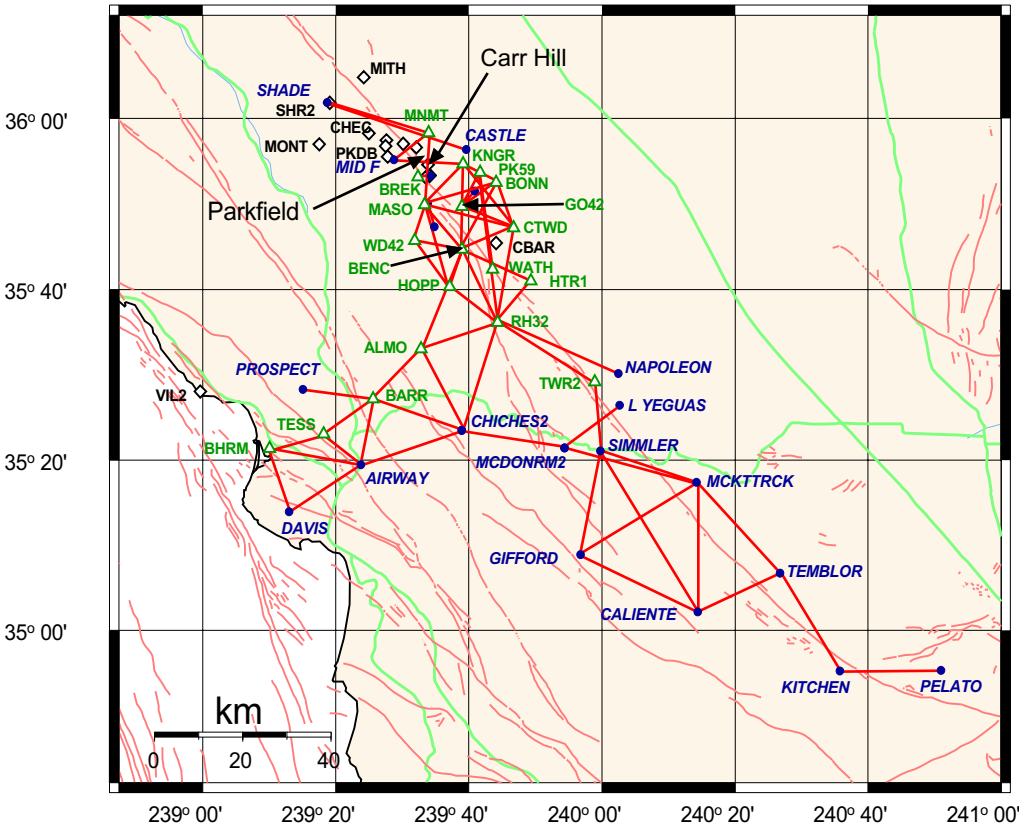

Figure 1: Parkfield area geodetic stations and trilateration lines used in this study. Circles = sites used for trilateration only (with italicized labels); diamonds = sites used for GPS only; triangles = sites used for trilateration and GPS (GPS station names used for labels). Town of Parkfield and Carr Hill are shown for reference. Not all sites are labeled, in the interest of map clarity.

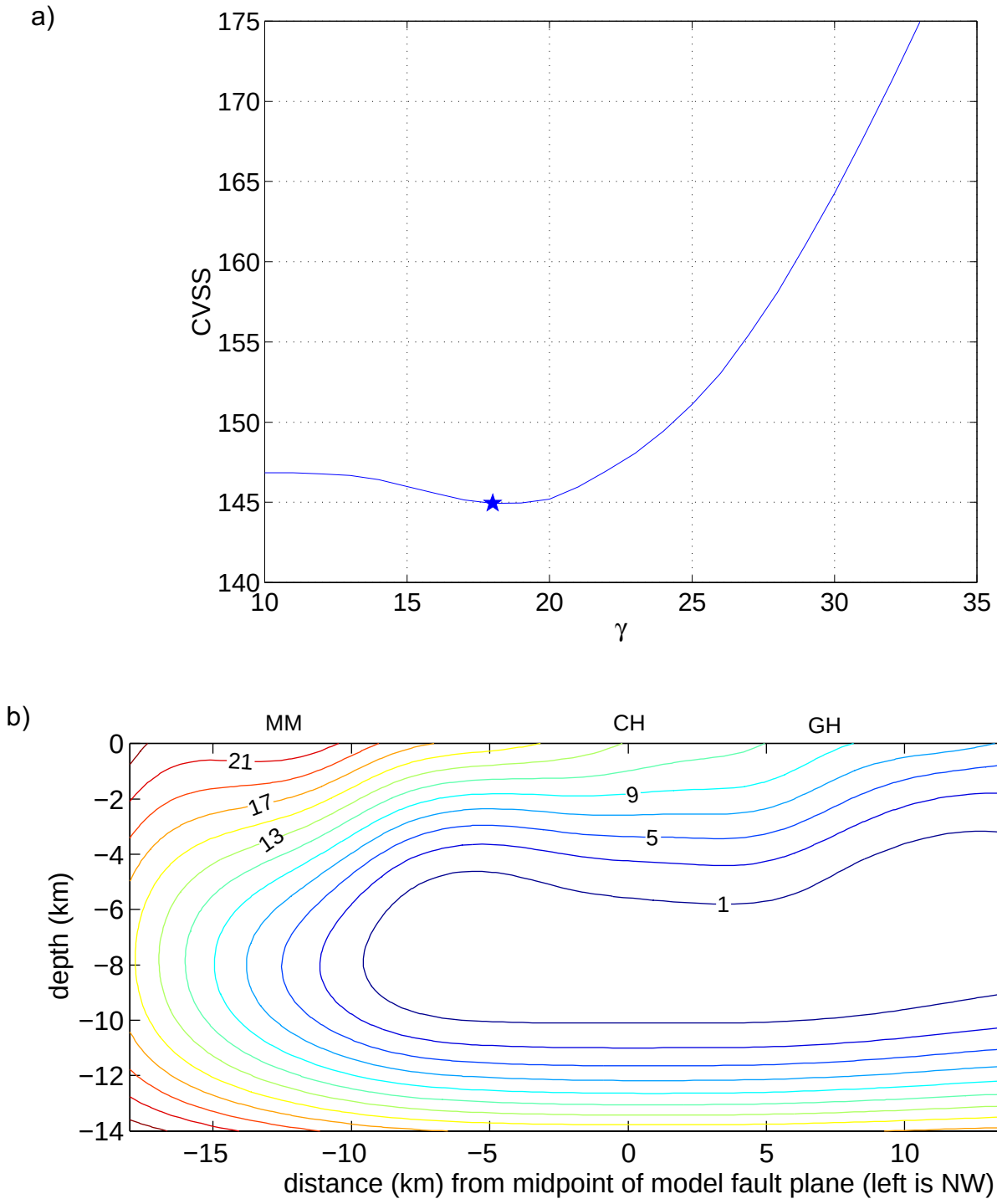

Figure 2: a) Cross validation sum of squares as a function of γ for NNLS inversions of trilateration data. Optimal value of γ is 18. b) Slip-rate distribution (mm/yr) based on NNLS inversion of trilateration data using γ = 18 and deep slip-rate = 32 mm/yr. MM indicates approximate location of Middle Mountain, CH indicates Carr Hill, and GH indicates Gold Hill.

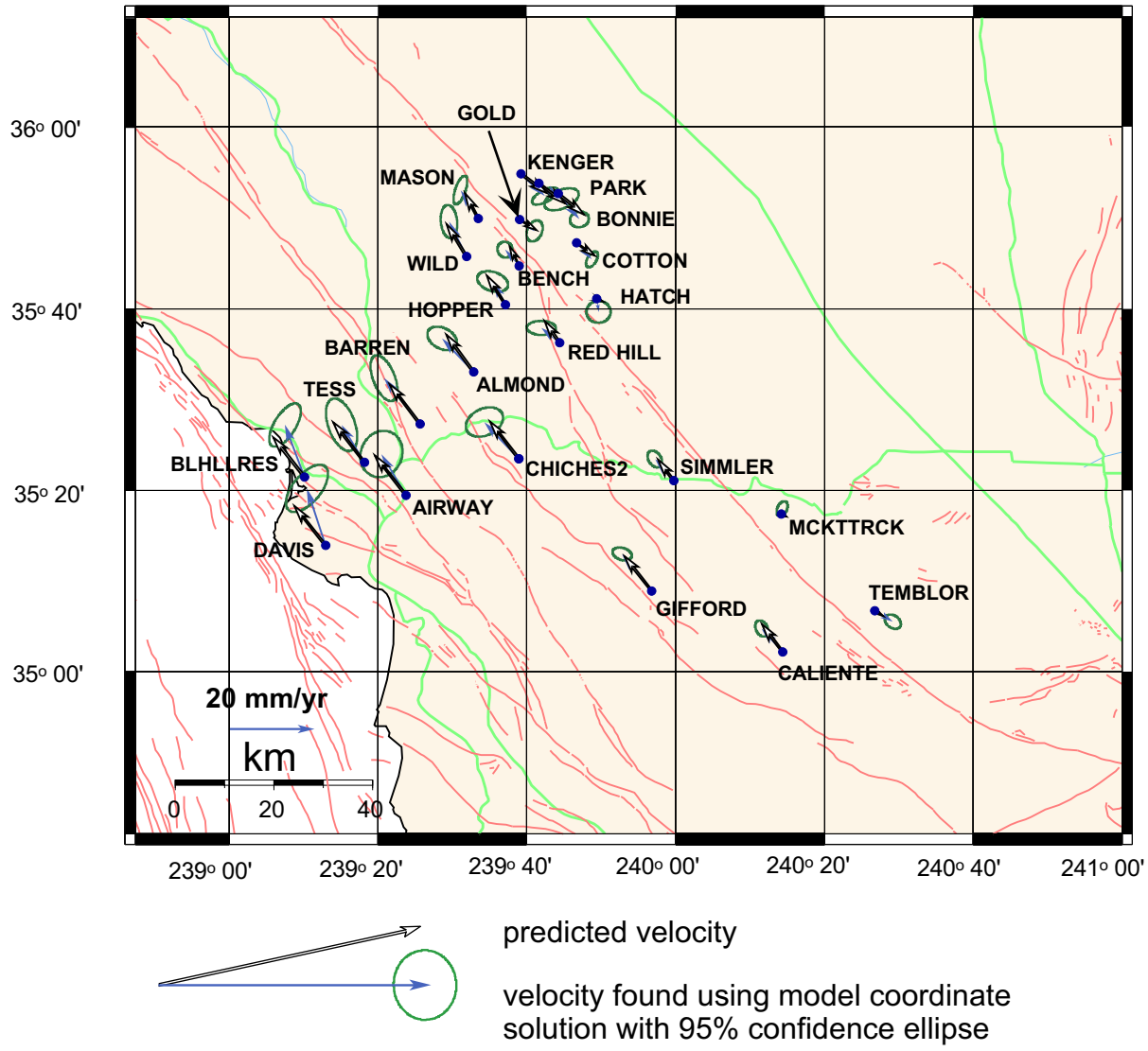

Figure 3: Velocities for trilateration sites. Predicted velocities are based on estimated slip distribution (found with $\gamma = 18$, deep slip-rate = 32 mm/yr, and transition depth = 14 km). Observed velocities are found using model coordinate solution (see text).

a)

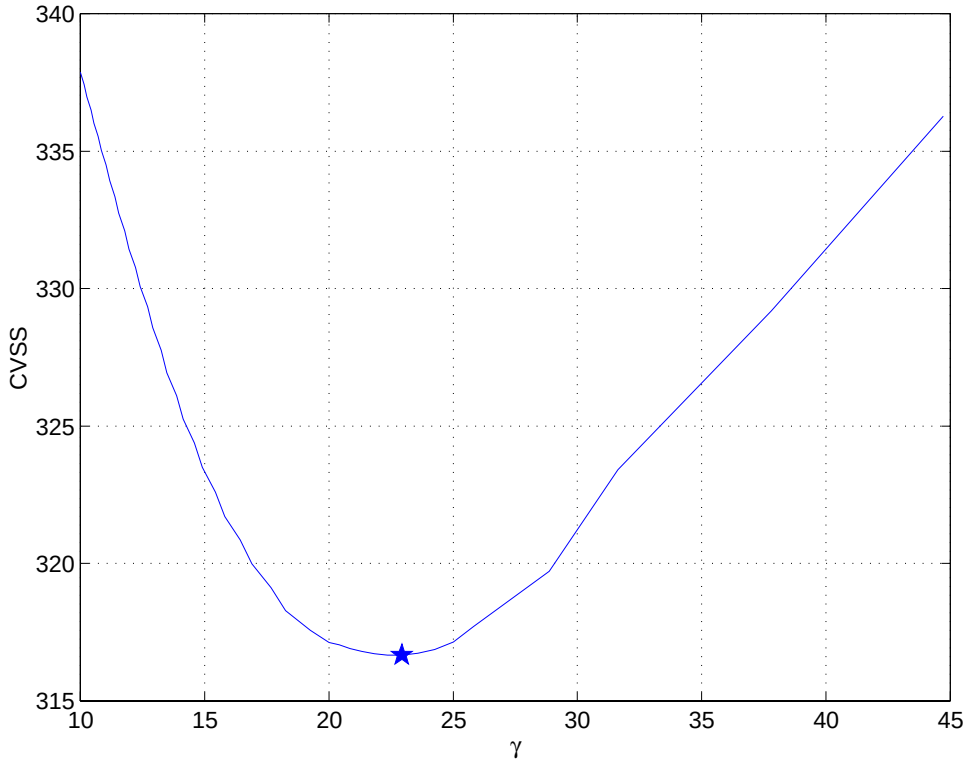

b)

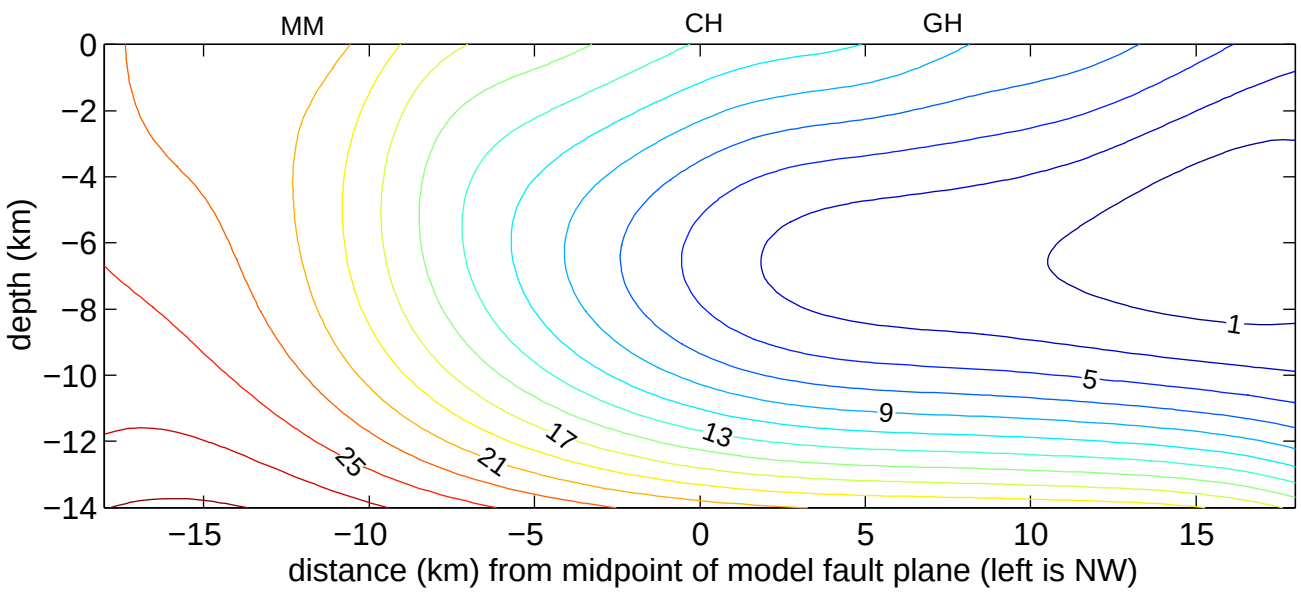

Figure 4: a) Cross validation sum of squares as a function of γ for NNLS inversions of GPS data. Optimal value of γ is 22.9. b) Slip-rate distribution (mm/yr) based on NNLS inversion of GPS data using γ = 22.9 and deep slip-rate = 32.6 mm/yr.

a)

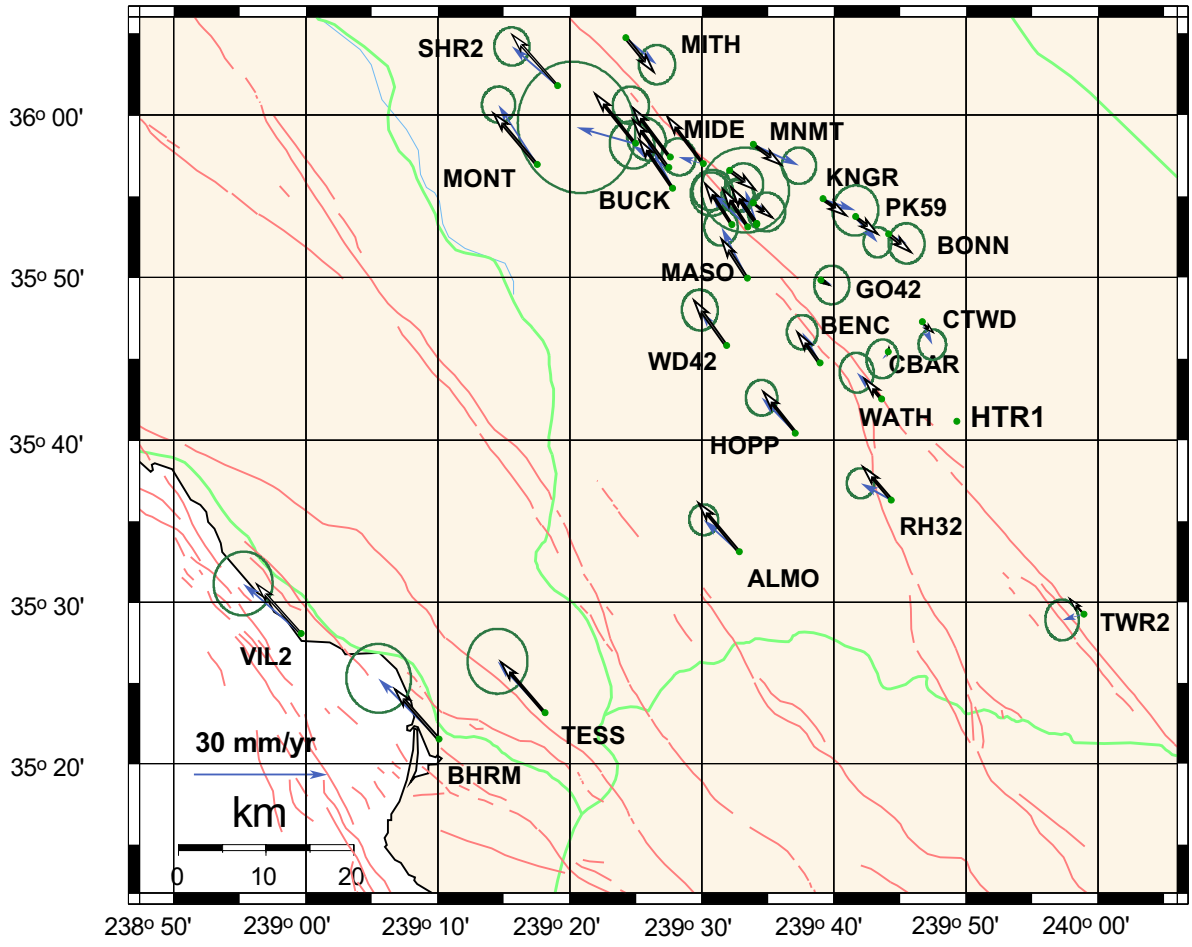

b)

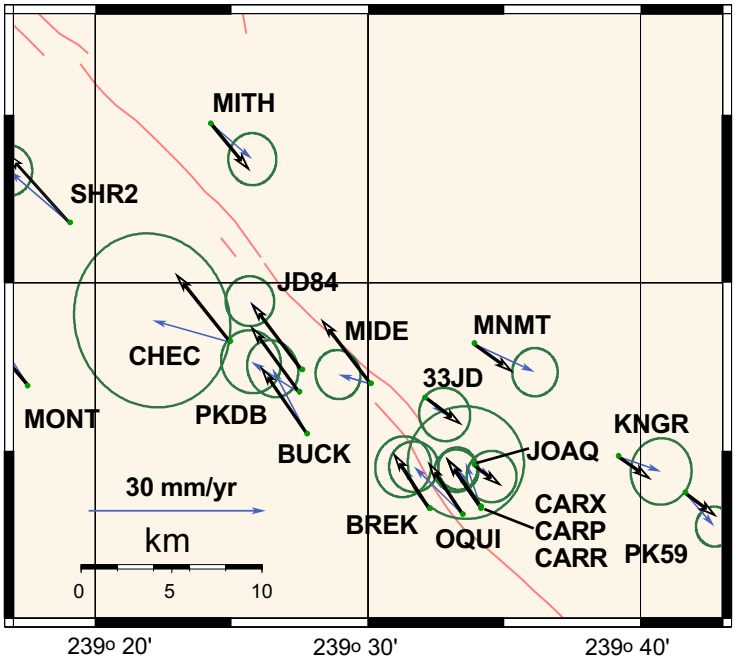

Figure 5: a) Velocities for GPS sites. Predicted velocities are based on estimated slip-rate distribution (found with $\gamma = 22.9$, deep slip-rate = 32.6 mm/yr, and transition depth = 14 km). b) close-up of area around Carr Hill. All velocities plotted relative to station HTR1.

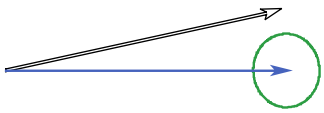

predicted velocity

observed velocity with 95% confidence ellipse

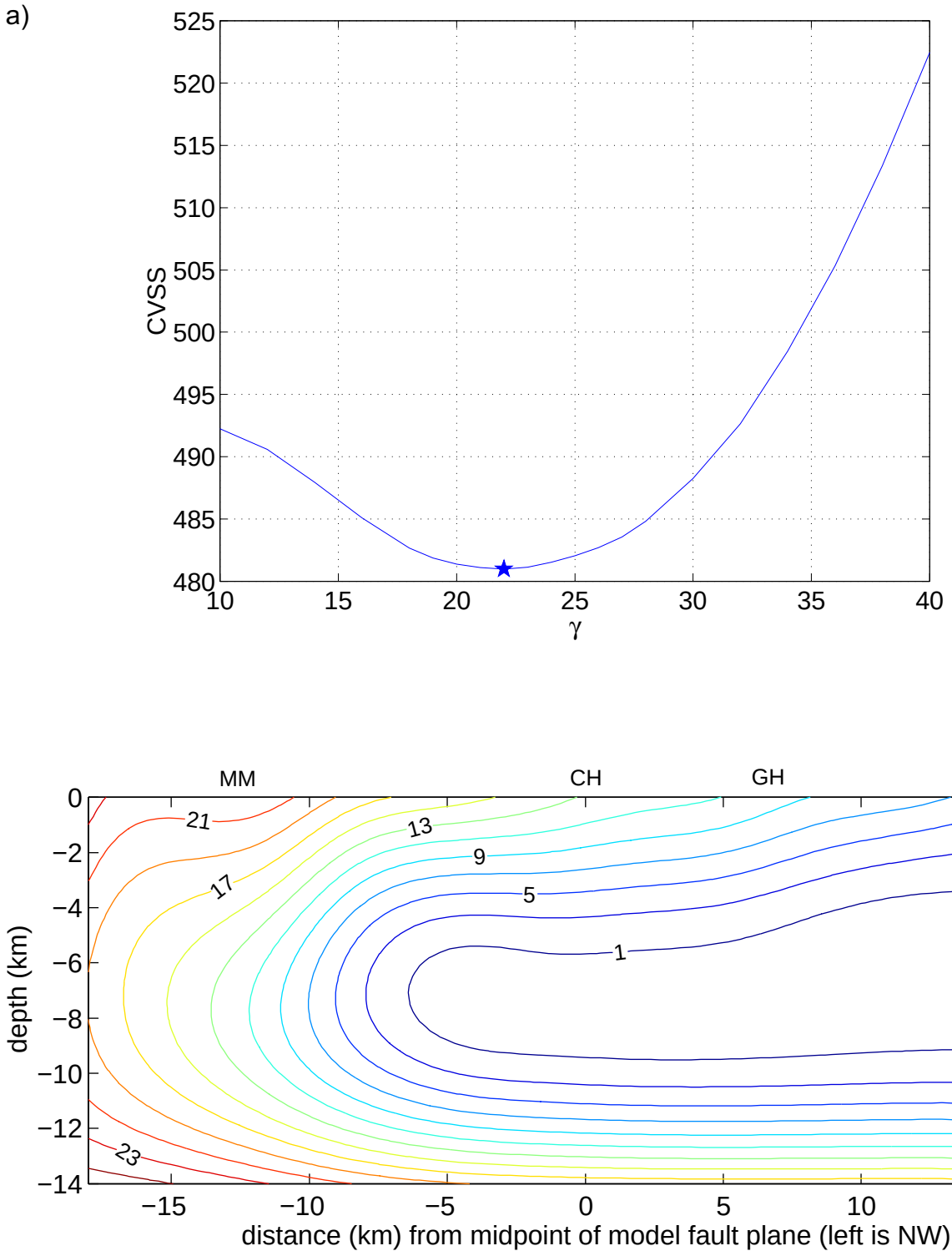

Figure 6: a) Cross validation sum of squares as a function of γ for NNLS inversions of trilateration and GPS data. Optimal value of γ is 22. b) Slip-rate distribution (mm/yr) based on NNLS inversion of trilateration and GPS data using $\gamma = 22$ and deep slip-rate = 33 mm/yr.

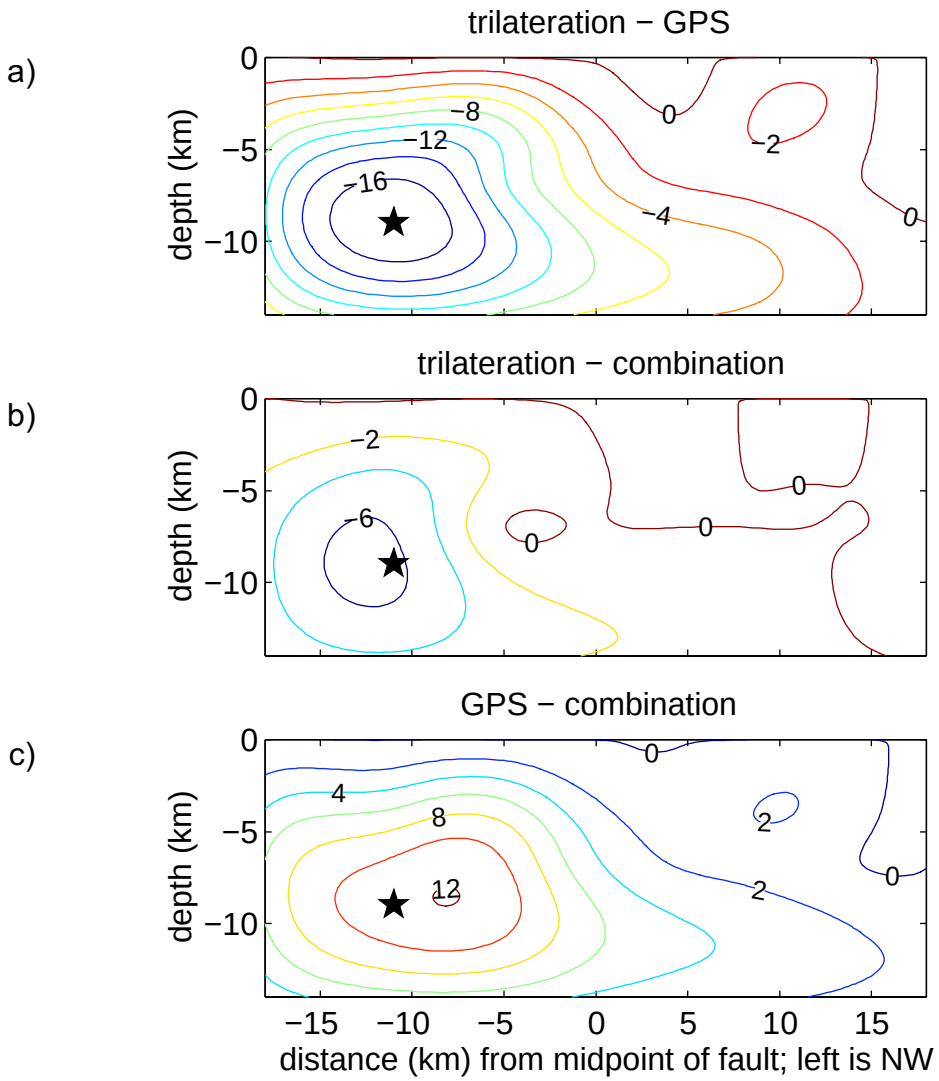

Figure 7: Difference in slip-rates estimated from different data sets. a) slip-rate based on trilateration data minus slip-rate based on GPS; b) slip-rate based on trilateration data minus slip-rate based on combination of both data sets; c) slip-rate based on GPS data minus slip-rate based on combination of both data sets. Stars indicate hypocenter of 1966 Parkfield earthquake.

Discussion:

Bill Bakun (USGS, M.P.): It looks like the model is limited by the extent to the southeast. Have you considered extending it farther to the southeast?

Jessica Murray: I haven't tried it, but it would be interesting to see.

Kevin Furlong (Penn State): Have you compared your slip model with the occurrence of microseismicity, e.g., do you see that where you have a locked zone, there is also a quiet area seismically?

Jessica Murray: I haven't plotted them on top of each other, but Harris and Segall have a paper about the correspondence, and it worked. This model is similar so I presume it would also work.